Lawrence Berkeley National Laboratory
Recent Work

**Title**
Analysis of nonisothermal injection and falloff tests in layered reservoirs

**Permalink**
https://escholarship.org/uc/item/7bf382g7

**Journal**
Geothermal Resources Council, 9

**Authors**
Halfman, Susan E.
Benson, Sally M.

**Publication Date**
1985

eScholarship.org Powered by the California Digital Library
University of California

LBL-19364

Lawrence Berkeley Laboratory
UNIVERSITY OF CALIFORNIA

EARTH SCIENCES DIVISION

RECEIVED
LAWRENCE
BERKELEY LABORATORY
MAY 22 1985
LIBRARY AND
DOCUMENTS SECTION

To be presented at the Geothermal Resources Council 1985 International Symposium on Geothermal Energy, Kailua Kona, HI, August 26-30, 1985

# ANALYSIS OF NONISOTHERMAL INJECTION AND FALLOFF TESTS IN LAYERED RESERVOIRS

S.E. Halfman and S.M. Benson

March 1985

TWO-WEEK LOAN COPY
This is a Library Circulating Copy
which may be borrowed for two weeks.

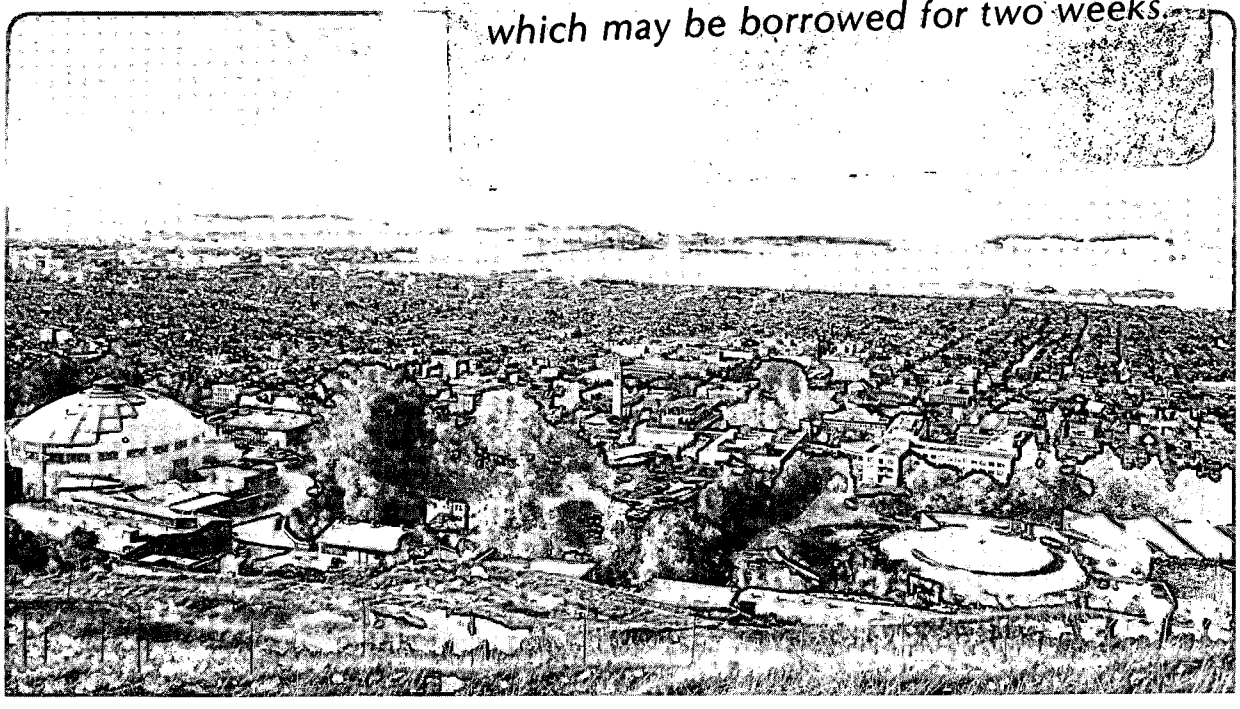

Prepared for the U.S. Department of Energy under Contract DE-AC03-76SF00098

LBL-19364
c.2

## DISCLAIMER

This document was prepared as an account of work sponsored by the United States Government. While this document is believed to contain correct information, neither the United States Government nor any agency thereof, nor the Regents of the University of California, nor any of their employees, makes any warranty, express or implied, or assumes any legal responsibility for the accuracy, completeness, or usefulness of any information, apparatus, product, or process disclosed, or represents that its use would not infringe privately owned rights. Reference herein to any specific commercial product, process, or service by its trade name, trademark, manufacturer, or otherwise, does not necessarily constitute or imply its endorsement, recommendation, or favoring by the United States Government or any agency thereof, or the Regents of the University of California. The views and opinions of authors expressed herein do not necessarily state or reflect those of the United States Government or any agency thereof or the Regents of the University of California.

# ANALYSIS OF NONISOTHERMAL INJECTION AND FALLOFF TESTS IN LAYERED RESERVOIRS

Susan E. Halfman and Sally M. Benson

Earth Sciences Division
Lawrence Berkeley Laboratory
University of California
Berkeley, California 94720

## ABSTRACT

The effects of reservoir layering and gravity segregation on nonisothermal injection and falloff tests are investigated. Results show that layering does not affect injection or falloff data if all the layers are permeable and accept fluids from the wellbore. In such cases, the average permeability, skin factor, and distance to the thermal front can be calculated using the techniques developed for homogeneous reservoirs. Special considerations have to be taken for cases where several layers are impermeable or are permeable but do not accept fluids of the well face. In the first case (impermeable layers), knowledge of the total thickness of the permeable layers is required for the existing techniques to be applied successfully. In the second case, the existing techniques cannot be appplied, but characteristic responses from injection and falloff test are seen; therefore, this case can be identified easily.

## INTRODUCTION

Pressure transient responses during nonisothermal injection and fall-off tests have been investigated by several authors in recent years. Bodvarsson and Tsang (1980) and Mangold et al. (1981) have shown that nonisothermal pressure transients depend on the fluid viscosity and density. Tsang and Tsang (1978) developed a semi-analytical solution for pressure transients affected by moving thermal fronts. Benson and Bodvarsson (1982) developed a method for calculating the skin factor from pressure transients in nonisothermal injection tests, and defined the conditions that result in composite reservoir or moving-front dominated behavior. In all of these cases, methods for calculating reservoir transmissivity, skin and apparent skin factors, and distance to the thermal front assume that the subsurface stratigraphy is homogeneous, and that the effects of gravity and heat conduction to the confining strata are negligible.

In general, the above assumptions are rarely realistic. For instance, the subsurface geology is often complex, and the presence of different lithologic layers affect the results of injection and falloff tests. In the present study, we analyze the effect of reservoir layering on nonisothermal pressure transients. The influence of gravity is also considered.

Two different models of the subsurface are used in this study. In the first model (the lithologic model), permeabilities of the subsurface layers are calculated from well log data. In the second model (the spinner model), permeabilities are calculated for productive zones interpreted from a spinner survey. The results of this study can be used as a basis for comparison of actual field injection and falloff tests.

A well from the East Mesa geothermal field was chosen for this study (Well 56-30). The subsurface stratigraphy is characterized by complex interfingering of marine and nonmarine sedimentary Late Tertiary and Quarternary deposits from the Colorado River (van de Kamp et al., 1978).

## APPROACH

For each of the two models considered (lithologic and spinner), the following conditions apply:

1) Each layer of the reservoir has constant porosity, compressibility, heat capacity, and thermal conductivity.

2) The layers are horizontal, areally infinite, and of constant thickness. The reservoir is bounded above and below by impermeable rock.

3) The reservoir is completely filled with slightly compressible liquid water.

4) Tilting (due to gravity) of the cold water front is neglected unless stated otherwise in Table 1.

5) The permeability of the layers in the reservoir is independent of temperature.

### Lithologic Model

In the lithologic model, the subsurface is divided into low and high permeability units. These groupings are determined by considering intervals that are predominately sandstone or shale. The computational mesh is generated on the basis of these layers. Permeabilities are assigned to each layer according to log-derived porosities.

Figure 1 shows the five layers chosen for the lithologic model. Layer 1 consists predominately of shales of comparatively high densities (low permeabilities). Layer 2 is comprised of interbedded sandstones and shales. Layers 3 and 5 consist predominately of sandstones, while layer 4, mainly of shales.

The permeabilities of each layer are calculated from porosities determined from the compensated formation density log. A porosity ($\phi$) is assigned to each layer. The permeability (k) of the first layer ($k_1$) is determined from

$$k_1 = 9.75 \times 10^{-12}\ m^3 / \sum_{i=1}^{5} \frac{\phi_i h_i}{\phi_1} \qquad (1)$$

and permeabilities for layers 2-5 are calculated by

$$k_i = \frac{\phi_i}{\phi_1} k_1 \qquad i = 2, \ldots, 5 \qquad (2)$$

The total kh of the producing interval (i.e., $9.75 \times 10^{-12}\ m^3$) was determined from interference testing (Narasimhan et al., 1978).

For the lithologic model, eight cases are considered (Table 1). Four of the cases (L1-L4) have different permeabilities assigned to each layer according to different assumptions about the subsurface fluid flow. In Case L1 (homogeneous reference case), the fluid is assumed to flow evenly into the subsurface. In Case L2, the fluid flow is assumed to be governed by the overall porosity of each layer. The permeabilities of each layer

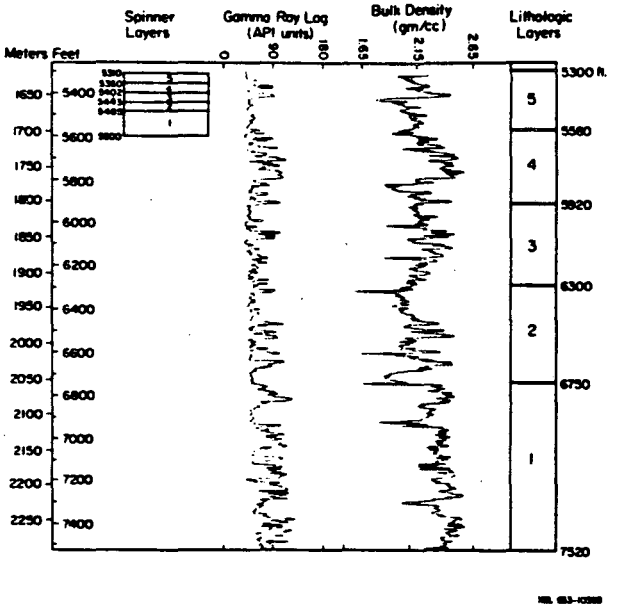


Figure 1. Columns for the lithologic and the spinner models representing the depth of the layers. The gamma-ray and compensated formation density logs show geologic characteristics associated with these layers.

are calculated from the averaged porosities of sandstones and shales within the layer. In Case L3, the fluid is assumed to flow only through the sandstone layers. The permeabilities are calculated from sandstone porosities averaged over the total thickness of each layer. In Case L4, the fluid is assumed to flow preferentially through the sandstones in layer 2. The permeability of layer 2 is calculated from averaged porosities of the sandstones in that layer (hence, a high permeability); averaged sandstone and shale porosities are used for lithologic layers 1, 3, 4, and 5 (lower permeabilities).

Because shales are often relatively impermeable, we consider three other cases, which are variations of Case L3. In Case L3C, fluid does not enter the predominately shaly layers (1 and 4) from the wellbore. However, the rocks are permeable enough for fluid to migrate into them beyond the wellbore. In this case, the permeabilities used in Case L3 are assigned to each layer, but layers 1 and 4 are disconnected from the wellbore. Case L3CG is the same as L3C, with the addition of gravity effects. In Case L3CI, layers 1 and 4 are considered to be completely impermeable (k = 0.00 md). The last case, Case L1G, is similar to L1, but gravity is added.

## Spinner Model

In the second model (spinner model), two primary productive intervals are identified from a spinner log (spinner layers 1 and 5 in Fig. 1). To create the same five-layer mesh as in the lithologic model, three nonproductive intervals are created (spinner layers 2, 3, and 4) between the two productive layers. Permeabilities for the two productive layers are calculated using the same method as in the lithologic model, however, the percentage of fluid is treated as the porosity parameter in Equation 2.

The fact that the two models are so different is surprising. The lithologic model essentially covers the entire perforated interval. On the other hand, the spinner model indicates that only a small fracture of the perforated interval produces fluids. No explanation for the discrepancy between the models is available at this time. However, it does indicate that interpretation of conventional logs may not be suitable for identifying productive intervals in the East Mesa geothermal field. On the other hand, the spinner survey may be influenced primarily by near-well conditions, and not provide representative values of the permeability distribution farther away from the wellbore.

## Numerical Model

The numerical simulator PT (Bodvarsson, 1981) is used to simulate the nonisothermal injection and falloff tests. The simulator is three-dimensional and solves the mass and energy transport equations for a liquid-saturated, heterogeneous, porous medium. It employes the "integrated finite difference" method for discretizing the medium and formulating the governing equations (Edwards, 1972). The set of linear equations is solved at each time step by direct means using a sparse matrix solver (Duff, 1977).

Table 1. Description of cases studies.

| Model | Case | Basis of Permeability Calculation for each layer | Reservoir Temp. (°C) | Injection Temp. (°C) | Permeability ($m^2 \times 10^{-14}$) Layer 1 | 2 | 3 | 4 | 5 |
|---|---|---|---|---|---|---|---|---|---|
| Lithologic | L1 | Assumed homogeneous case | 170 | 50 | 1.44 for 1 layer assumed | | | | |
| | L2 | Averaged sandstone and shale porosities | 170 | 50 | 1.018 | 1.900 | 1.526 | 1.323 | 1.900 |
| | L3 | Average sandstone layers | 170 | 50 | 1.079 | 1.815 | 1.373 | 1.618 | 1.716 |
| | L4 | 1) Layers 1, 3-5 from averaged sandstone and shale porosities<br>2) Layer 2 from averaged sandstone porosities | 170 | 50 | 0.989 | 2.045 | 1.484 | 1.286 | 1.847 |
| | L1G | Same as L1, gravity effects included | 155 | 50 | | | | | |
| | L3C | Same as L4, except layers 1 and 4 are disconnected from the wellbore | 155 | 50 | | | | | |
| | L3CG | Same as L3C, gravity effects included | 155 | 50 | | | | | |
| | L3CI | Similar to L3C, except $K_1$ and $k_4$ equal zero | 155 | 50 | 0.000 | 3.192 | 2.416 | 0.00 | 3.020 |
| Spinner | S1 | Production rates based on simplified spinner data | 155 | 50 | 18.410 | 0 | 0 | 0 | 21.655 |

The simulator allows for temperature- and/or pressure-dependent fluid and rock properties. The water density is calculated as a function of pressure and temperature, using a polynomial approximation. Water viscosity is calculated as a function of temperature using an exponential expression. The simulator has been validated against many analytical solutions as well as field experiments (Doughty et al., 1983). A detailed description of the simulator is given by Bodvarsson (1981).

Grid Size and Time Steps

A five-layer radial mesh with a realistic wellbore radius of 0.1 m is used in the study. Figure 1 shows the thickness of each of the five layers for both models. In the lithologic model, layers 1-5 are 234.7, 137.2, 115.8, 103.6, and 85.3 m thick, respectively. In the spinner model, layers 1-5 are 35.0, 12.7, 12.7, 12.7, and 15.3 m thick, respectively. Close to the well very fine elements (20 x .02 m, 10 x 0.05 m, 6 x 0.1 m, 17 x 0.2 m, 2 x 0.4 m, 1 x 0.5 m, and 1 x 0.6 m) are used for accurate modeling of temperature variations during injection and falloff. Farther away from the well, the mesh spacing increases logarithmically for accurate modeling of the pressure response. A total of 410 elements (5 layers x 82) are used. The outer boundary of the mesh, (r = 100,000 m) is sufficiently distant so that boundary effects do not influence the calculations.

The time steps are automatically selected by the numerical code, based upon user-specified criteria for the maximum allowable pressure and temperature changes during each time step. For most runs, maximum allowable pressure and temperature changes of 1 bar and 1°C are specified.

METHOD

In this study, constant rate injection and falloff tests are simulated for 0.5, 1, and 5 days and for 10 and 20 days where indicated in Table 2. Transmissivity, apparent skin factors, and the distance to the thermal fronts are calculated for each case studied using the methods developed for homogeneous reservoirs. Benson and Bodvarsson (1982) and Benson (1984) give detailed discussions of the theoretical considerations in nonisothermal injection testing. For clarity, brief descriptions of nonisothermal injection and falloff tests are given below.

Figure 2 illustrates the pressure transient response during a typical nonisothermal injection test. In this case, cold water (50°C) is injected into a 170°C reservoir. At early times, the pressure transients correspond to the temperature of the geothermal reservoir fluids as shown by the first slope in Figure 2. At later times the pressure transients respond to the cooler injected fluids as indicated by the second slope. The kh can be calculated from (in S.I. units - mks)

Table 2. Results of cases studied.

| Case | Time (Day) | $p_{wf}$ ($10^5$Pa) | $p_{1s}$ ($10^6$Pa) | m ($10^5$Pa/cy) | kh ($10^{-12}m^3$) | $\phi ch$ ($10^{-7}m^3$) | $\mu$ ($10^{-4}$Pa) | $r_w^2$ ($10^{-2}$ $m^2$) | $s_a$ | $s_f$ | $r_f$ (m) |
|---|---|---|---|---|---|---|---|---|---|---|---|
| L1 | 1/2 | 1.030 | 4.61 | 1.005 | 9.566 | 1.49 | 1.585 | 1.00 | 4.2 | 4.9 | 1.0 |
| | 1 | 1.122 | 4.98 | 1.005 | 9.566 | 1.49 | 1.585 | 1.00 | 4.9 | 5.6 | 1.4 |
| | 5 | 1.339 | 5.69 | 1.005 | 9.566 | 1.49 | 1.595 | 1.00 | 6.5 | 7.2 | 2.9 |
| L2 | 1/2 | 1.030 | 4.71 | 1.02 | 9.426 | 1.49 | 1.585 | 1.00 | 4.1 | 4.8 | 9.5 |
| | 1 | 1.126 | 4.98 | 9.85 | 9.760 | 1.49 | 1.585 | 1.00 | 5.1 | 5.8 | 1.5 |
| | 5 | 1.341 | 5.66 | 1.00 | 9.614 | 1.49 | 1.585 | 1.00 | 6.6 | 7.3 | 3.1 |
| L3 | 1/2 | 1.031 | 4.72 | 1.01 | 9.519 | 1.49 | 1.585 | 1.00 | 4.1 | 4.8 | .95 |
| | 1 | 1.125 | 4.98 | 1.01 | 9.566 | 1.49 | 1.585 | 1.00 | 4.9 | 5.8 | 1.4 |
| | 5 | 1.342 | 5.72 | 1.01 | 9.519 | 1.49 | 1.585 | 1.00 | 6.5 | 7.3 | 3.2 |
| L4 | 1/2 | 1.033 | 4.67 | 1.01 | 9.519 | 1.49 | 1.585 | 1.00 | 4.2 | 4.9 | 1.0 |
| | 1 | 1.125 | 5.05 | 1.00 | 9.614 | 1.49 | 1.585 | 1.00 | 4.9 | 5.6 | 1.4 |
| | 5 | 1.343 | 5.66 | 1.00 | 9.614 | 1.49 | 1.585 | 1.00 | 6.7 | 7.4 | 3.2 |
| L1G | 1/2 | 1.240 | 6.75 | 1.09 | 9.587 | 1.49 | 1.749 | 1.00 | 3.7 | 4.3 | 1.0 |
| | 1 | 1.334 | 7.12 | 1.11 | 9.414 | 1.49 | 1.749 | 1.00 | 4.2 | 4.8 | 1.3 |
| | 5 | 1.552 | 7.13 | 1.11 | 9.414 | 1.49 | 1.749 | 1.00 | 5.7 | 6.3 | 2.9 |
| | 10 | 1.646 | 8.22 | 1.11 | 9.414 | 1.49 | 1.749 | 1.00 | 6.4 | 7.0 | 4.1 |
| L3C | 1/2 | 1.968 | 7.43 | 1.62 | 6.445 | 1.49 | 1.749 | 1.00 | 6.7 | | |
| | 1 | 2.107 | 6.86 | 1.39 | 6.445 | 1.49 | 1.749 | 1.00 | 9.7 | | |
| | 5 | 2.439 | 5.90 | 1.15 | 9.080 | 1.49 | 1.749 | 1.00 | 16.3 | | |
| | 10 | 2.575 | 6.39 | 1.07 | 9.759 | 1.49 | 1.749 | 1.00 | 17.4 | | |
| | 20 | 2.709 | 6.74 | 1.08 | 9.669 | 1.49 | 1.749 | 1.00 | 19.4 | | |
| L3CG | 1/2 | 2.158 | 8.94 | 1.56 | 6.705 | 1.49 | 1.749 | 1.00 | 7.2 | | |
| | 1 | 2.301 | 8.77 | 1.44 | 7.264 | 1.49 | 1.749 | 1.00 | 9.3 | | |
| | 5 | 2.630 | 7.93 | 1.08 | 9.685 | 1.49 | 1.749 | 1.00 | 17.3 | | |
| | 10 | 2.768 | 8.02 | 1.05 | 9.962 | 1.49 | 1.749 | 1.00 | 19.3 | | |
| L3C1 | 1/2 | 1.158 | 4.99 | 1.07 | 9.759 | 1.49 | 1.749 | 1.00 | 4.9 | 5.1 | 1.5 |
| | 1 | 1.248 | 5.32 | 1.07 | 9.759 | 1.49 | 1.749 | 1.00 | 5.5 | 6.7 | 2.1 |
| | 5 | 1.464 | 6.06 | 1.06 | 9.852 | 1.49 | 1.749 | 1.00 | 7.1 | 7.3 | 4.9 |
| | 10 | 1.557 | 6.46 | 1.07 | 9.759 | 1.49 | 1.749 | 1.00 | 7.6 | 7.8 | 6.3 |
| S1 | 1/2 | 1.439 | 5.10 | 1.09 | 9.580 | .110 | 1.749 | 1.00 | 6.3 | 7.0 | 4.1 |
| | 1 | 1.534 | 5.39 | 1.08 | 9.670 | .110 | 1.749 | 1.00 | 7.1 | 7.8 | 6.3 |
| | 5 | 1.744 | 6.26 | 1.10 | 9.493 | .110 | 1.749 | 1.00 | 8.2 | 9.1 | 12.7 |
| | 10 | 1.828 | 6.52 | 1.10 | 9.493 | .110 | 1.749 | 1.00 | 8.8 | 9.0 | 15.7 |

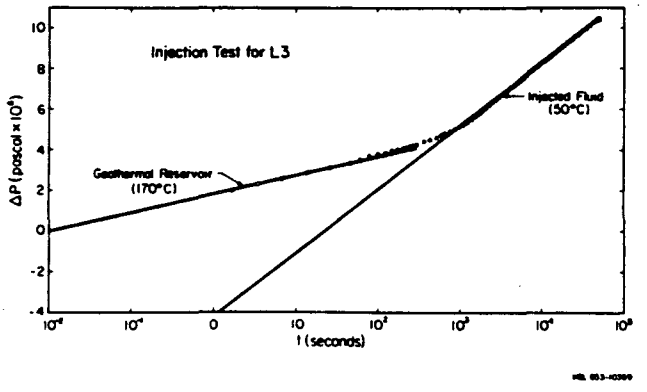


Figure 2. Pressure transient data for 50°C injection into a 170°C reservoir for Case L3.

$$kh = \frac{0.183q\mu}{m\rho} \quad (3)$$

where the appropriate viscosity ($\mu$) and fluid density ($\rho$) are determined by procedures developed by Benson and Bodvarson (1982) and Benson (1982).

It is important to note that if a "cold spot" exists around the well prior to injection, the pressure transient response will be very different (Bodvarsson, 1981; Benson and Bodvarsson, 1982). For this reason, it is desirable to analyze pressure falloff data, because only one type of pressure transient response is possible (due to nonisothermal conditions).

After shutting in the well (falloff), the reservoir behaves as a two-fluid composite reservoir, with the colder injected fluids surrounding the

wellbore and the in situ reservoir fluid in the outer region. A typical pressure transient response to falloff tests is shown in Figure 3. The first slope corresponds to the fluids around the well and the second slope to the in situ geothermal fluids.

Theoretically, kh can be calculated from a pressure falloff test by using either the first or second semi-log straight line, if the correct set of fluid properties is used. However, since the first semi-log straight line will often be obscured by wellbore storage, the most reliable approach is to use the second semi-log straight line (i.e., not the very early time data). In this case

$$kh = \frac{0.183 q \mu_o}{m_o \rho_o} \tag{4}$$

The apparent skin factor of the well ($s_a$) is calculated by

$$s_a = 1.151 \left( \frac{p_{1s} - p_{wf}}{m_o} - \log \frac{k_o}{\phi_o \mu_o c_o r_w^2} - 0.351 \right) \tag{5}$$

The apparent skin factor has two components, one due to the actual mechanical skin factor of the well ($s_m$), and another one due to the cold spot around the well (fluid skin factor). The fluid skin factor is defined as

$$s_f = \left( \frac{\mu_i}{\mu_o} \frac{\rho_o}{\rho_i} - 1 \right) \ln \frac{r_f}{r_w} \tag{6}$$

By conducting a series of falloff tests, it is possible to distinguish between the actual mechanical skin factor the fluid skin factor (Benson, 1982). To do this, a plot of $s_a$ versus the logarithm of the cumulative injection volume (C) is prepared. The slope of the line drawn through the data points is given by

$$n = 1.151 \left( \frac{\mu_i}{\mu_o} \frac{\rho_o}{\rho_i} - 1 \right) \tag{7}$$

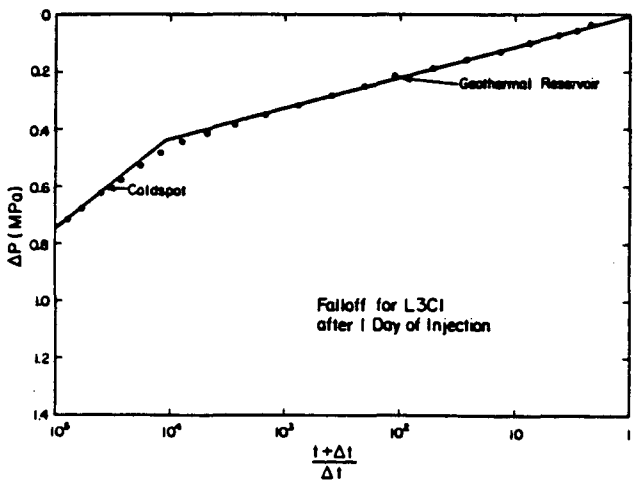


Figure 3. Pressure falloff data after injection (50°C into 150°C) reservoir for Case L3CI.

By extrapolating the line (n) back to the point where $C = \pi h r_w^2$, an estimate of the mechnical skin factor can be obtained:

$$s_m = \frac{\mu_o \rho_i}{\mu_i \rho_o} \left( s_a (\pi h r_w^2) - n \log \frac{\rho_w c_w}{\rho_a c_a} \right) \tag{8}$$

The fluid skin factor due to the cold spot around the well can than be calculated by

$$s_f(C) = s_a(C) - \frac{\mu_i}{\mu_o} \frac{\rho_o}{\rho_i} s_m \tag{9}$$

From the value of $s_f$ and n, the distance to the cold front can be calculated by

$$r_f = r_w \exp \left( 1.151 \frac{s_f}{n} \right) \tag{10}$$

To address the question of the applicability of these methods to layered reservoirs; Σkh values, apparent skin factors, mechanical skin factors, and distance to the thermal front are calculated for all of the falloff tests, using the methodology outlined above. The following section discusses the results of these calculations.

## RESULTS

For each of the cases in which fluid is injected along the entire length of the wellbore (Cases L1-L4, L1G), the pressure transient response is indistinguishable from the homogeneous reference case (L1). For example, the injection pressure transients for Case L3 (see Fig. 3), are identical to those of the homogeneous reference case. However, in this case, it is the Σkh that can be determined from the slope of the semi-log straight line. The validity of this conclusion is demonstrated by the excellent agreement of the Σkh values calculated for each of these cases (see column 6, Table 2).

Apparent skin factors ($s_a$) are also calculated for the falloff tests after 0.5, 1, and 5 days of simulated injection. The calculated values are tabulated in Table 2 (column 10) and plotted in Figure 4 (L3) and Figure 5. As in the homogeneous reference case, they fall on a semi-log straight line when plotted as a function of the cumulative injection. The slope of the line (2.4/cycle) is the same as that predicted by Equation 7. Case L1G is also equivalent to a homogeneous case, however for this case the reservoir is 155°C, instead of 170°C; therefore, the apparent skin factors are correspondingly lower (see Eq. 6).

Using Equations 5 to 10, values of the fluid skin and the distance to the thermal front are calculated and tabulated in Table 2. In each case, the values of the fluid skin factor and the distance to the thermal front are essentially identical to the values calculated for the homogeneous reference case. The explanation for the lack of sensitivity to reservoir layering and gravity segregation is illustrated in Figures 6 and 7, which show the distance to the thermal front for each of the cases considered. Although the distance to the thermal front is different in each layer, the relatively small variation

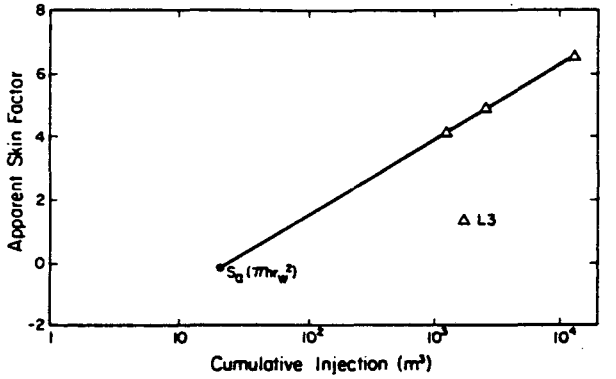


Figure 4. Apparent skin factor vs cumulative injection for Case L3.

in the permeability and the short test periods used for this study do not result in sufficient differences to influence the overall pressure transient response. Therefore, it is the average distance to the thermal front (i.e., the equivalent of the homogeneous case), that influences the pressure buildup resulting from the cold water around the well. Comparison between the calculated values of the distance to the thermal front (Table 2) and the average of the actual values shown in Figures 6 and 7 shows excellent agreement.

Of the remaining cases, two are influenced by the effects of impermeable reservoir layers (L3CI and S1) and two by a wellbore that partially penetrates the reservoir (L3C and L3CG). For the cases with impermeable layers (L3CI, S1), the pressure transient responses are similar to those discussed above. That is, the injection and falloff pressure transients have the same basic characteristics as shown in Figures 2 and 3. The Σkh can be calculated from the semi-log slope of the late-

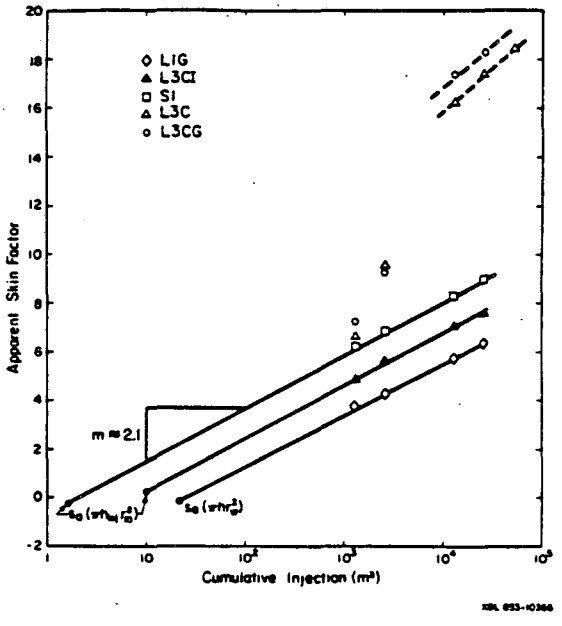


Figure 5. Apparent skin factor vs cumulative injection for Cases L1G, L3CI, S1, L3C, and L3CG.

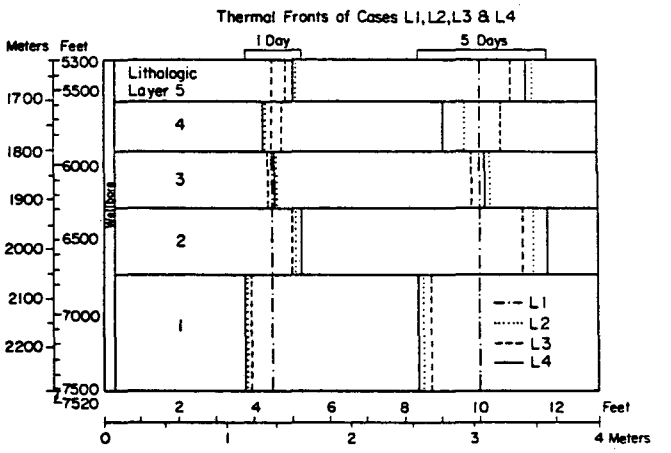


Figure 6. Distances to the thermal fronts after 1 and 5 days of injection Cases L1, L2, L3, and L4.

time data falloff data by using Equation 4. The apparent skin factors are calculated by Equation 5. The calculated values of Σkh and $s_a$ for these two cases are listed in Table 2. As in Cases L1-L4, the values of $s_a$, when plotted as a function of log (C), fall on a straight line whose slope is given by Equation 7. However, as shown in Figure 5, the values of $s_a$ are higher than in the cases where fluid is injected along the entire length of the wellbore (Case L1G). This is the result of the faster rate at which the cold fluid migrates along the thinner layers.

It appears that this may provide a method of detecting preferential migration of cold fluid along several thin layers, rather than along the entire interval. However, a problem arises in evaluating the actual distance to the thermal front. The method used for homogeneous reservoirs requires that $s_a$ be evaluated when $C = \pi h r_w^2$, where h is assumed to be equal to the entire open interval of the well. If fluid is not injected along the entire length of the well, what is the appropriate choice of h?

Theoretical considerations indicate that the thickness ($h_{inj}$) of formation that accepts fluid at the well face is the appropriate value to use. In order to have an accurate value of $h_{inj}$, a spinner survey is required. If this is available, the correct average distance to the thermal front can be calculated using Equation 10. On the other hand, if an incorrect value of $h_{inj}$ is used, (i.e., the entire open interval), the distance to the thermal front will be underestimated and a positive skin factor (see Eq. 8) will be calculated.

For the two remaining cases (L3C and L3CG), the influence of the partially penetrating well is very significant. Instead of observing the two-slope behavior typical of nonisothermal injection and falloff (Figs. 2 and 3), the response is complicated by the effects of crossflow, created by the partially penetrating wellbore. Pressure falloffs (after 1 and 10 days of injection) for Case L3C are shown in Figure 8. The early-time response is influenced by the cold fluid around the well and the kh corresponds to the thickness of only those layers that are open

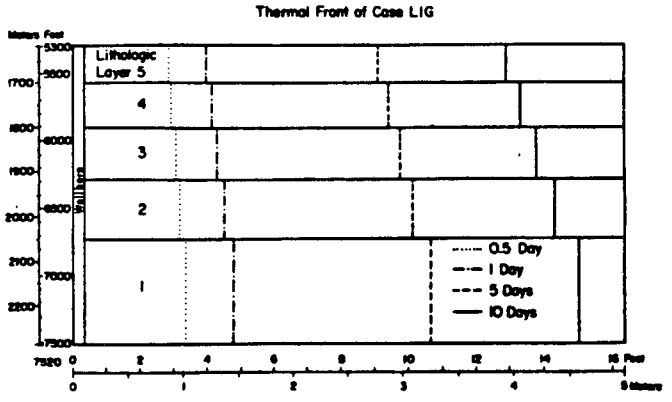


Figure 7. Distances to the thermal fronts after 0.5, 1, 5, and 10 days of injection for Case L1G.

to the well. During intermediate times, a transition period is created by the effects of partial penetration. At very large times, the total kh and fluid properties of the reservoir govern the response. However, as is shown by the falloff after 1 day in Figure 8, the final semi-log straight line (corresponding to the entire reservoir thickness) may not develop. The result of this long transitional period is evident from the wide range of kh values calculated from the 0.5, 1, 5, and 10 day injection cases. Until the 10-day falloff test, the correct value of $\Sigma kh$ is not obtained. Furthermore, the $\Sigma kh$ calculated from the short term tests (0.5 and 1 day), are not even the correct values for the layers penetrated by the well.

The influence of partial penetration is also apparent in the calculated skin factors (see Table 2). For the two short tests (1/2 and 1 day), the apparent skin factors are consistent with expected fluid skin values. However, for the 5 and 10 day tests, very large skin values are calculated (i.e., 16-19). The large apparent skin factors are the sum of the pseudo-skin factor resulting from partial penetration (Brons and Marting, 1961) and the fluid skin factor. The apparent skin factors for Cases L3CG and L3C are plotted as a function of log (C) in

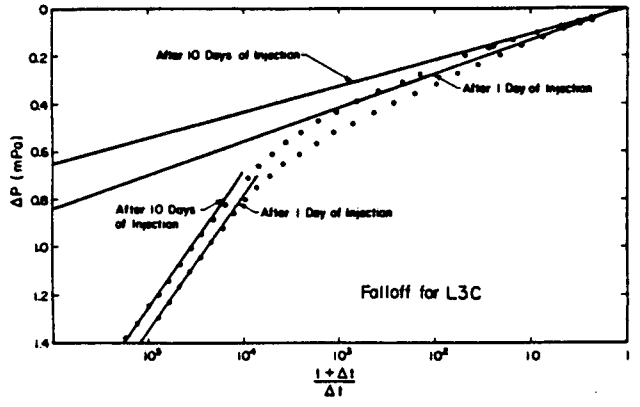


Figure 8. Pressure falloff data after 1 and 10 days of injection for Case L3C.

Figure 5. Unlike all of the previous cases, the slopes on the lines through the data points are not given by Equation 7. This is expected, in light of the complication arising from the effects of partial penetration. Obviously, if the distance to the thermal front or the mechanical skin factor is calculated by the procedure discussed previously, erroneous values are obtained.

## SUMMARY AND CONCLUSIONS

The influence of reservoir layering and gravity segregation on nonisothermal injection and falloff tests has been investigated. Results of the study show that if the wellbore fully penetrates the reservoir, the $\Sigma kh$, the mechanical skin factor of the well, and the average distance to the thermal front can be calculated. On the other hand, if only part of the reservoir is intersected by the injection well, or if only some of the layers accept fluid, interpretation of the data is complicated by these factors.

If the high permeability layers are separated by impermeable layers, the injection and falloff pressure responses have the same character as those of a homogeneous system. In this case, the $\Sigma kh$ can be calculated using conventional methods. However, in order to calculate the mechanical skin factor of the well and the average distance to the thermal front, an accurate estimate of the thickness of the permeable layers is required. Only if this is available can accurate values of these two parameters be obtained.

The situation is very different for wells that partially penetrate the reservoir. In these cases, the influence of cross flow and the resulting transiton period strongly affect the pressure transient response. The $\Sigma kh$ values, mechanical skin factor and distance to the thermal front will all be calculated incorrectly from short term tests (up to ten days for the cases considered here). Furthermore, in the analysis of subsequent tests, all of the parameters may appear to change (i.e., large increases in the apparent skin factor). If misinterpreted, these changes would lead one to believe that formation or wellbore damage occurred during injection. Fortunately, carefully controlled tests of sufficient duration can be used to detect this type of situation.

Injection and falloff field tests should be done for Well 56-30 to compare the field results with the results from this study. Only then will it be possible to determine the influence of each of these factors.

## ACKNOWLEDGEMENT

We would like to thank M. J. Lippmann and K. Pruess for reviewing this manuscript. This work was supported by the Assistant Secretary for Conservation and Renewable Energy, Office of Renewable Technology, Division of Geothermal and Hydropower Technologies of the U.S. Department of Energy under Contract No. DE-AC03-76SF00098.

NOMENCLATURE

| | |
|---|---|
| $C$ | cumulative injection ($m^3$) |
| $h$ | total thickness of perforated interval (m) |
| $h_{inj}$ | thickness of total injected interval(s) (m) |
| $k$ | permeability ($m^3$) |
| $m$ | slope of $\Delta p$ vs log $[(t + \Delta t)/\Delta t]$ ($P_a$/cycle) |
| $n$ | slope on $s_a$ vs log C straight line |
| $p$ | pressure ($P_a$) |
| $p_{1s}$ | extrapolated pressure at 1 s on a P vs log t plot |
| $p_{wf}$ | flowing pressure ($P_a$) |
| $q$ | mass flow rate (kg/s) |
| $r_f$ | radius to the thermal front (m) |
| $r_w$ | radius of wellbore (m) |
| $s_a$ | apparent skin factor |
| $s_f$ | fluid skin factor |
| $s_m$ | mechanical skin factor |
| $s_a(\pi h r_w^2)$ | apparent skin facotr evaluated at $\pi h r_w^2$ |
| $s_a(\pi h_{inj}\ r_w^2)$ | apparent skin factor evaluated at $\pi h_{inj}\ r_w^2$ |
| $t$ | time (s) |

Greek Letters

| | |
|---|---|
| $\rho$ | density ($kg/m^3$) |
| $\mu$ | dynamic viscosity ($p_a$.s) |

Subscripts

| | |
|---|---|
| i | inner region |
| o | outer region |

REFERENCES


Benson, S. M., 1984. Analysis of injection tests in liquid dominated geothermal systems, (M.S. Thesis) University of California, Berkeley, California.

Benson, S. M., 1982. Interpretation of nonisothermal step-rate injection tests. In Proceedings on the Eight Workshop on Geothermal Reservoir Engineering, December 12-14, 1982, Stanford, California, p. 103-109.

Benson, S. M. and Bodvarsson, G. S. 1982. Nonisothermal effects during injection falloff tests. SPE paper 11137, presented at the 57th Annual Meeting of the Society of Petroleum Engineers, New Orleans, Louisiana.

Bodvarsson, G. S., 1981. Mathematical modeling of the behavior of geothermal systems under exploitation (Ph.D. dissertation), Lawrence Berkeley Laboratory report LBL-13937.

Bodvarsson, G. S. and Tsang, C. F., 1980. Thermal effects in the analysis of fractured reservoir. In 3rd Invitational Well Testing Symposium. Lawrence Berkeley Laboratory report, LBL-12076, p. 110-119.

Brons, F., and Marting, V. E., 1961. The effect of restricted fluid entry on well productivity. Journal of Petroleum Technology, (Feb., 1961), Trans., AIME, 222.

Doughty, C., Buscheck, T. A., and Tsang, C. F., 1983. Prediction and analysis of a field experiment on a multi-layered aquifer thermal energy storage system with strong bouyancy flow. Water Resources Research, Vol. 19, No. 5, p. 1307-1315.

Duff, T. S., 1977. MA28 - A set of Fortran subroutines for sparse unsymmetric linear equations: Harwell Report AERE-R 8730, Great Britain.

Edwards, A. L., 1972. TRUMP: A computer program for transient and steady state temperature distribution in multidimensional systems. Lawrence Livermore Laboratory report, UCRL-14754, Rev. 3.

Mangold, D. C., Tsang, C. F., Lippmann, M. J., and Witherspoon, P. A., 1981. A study of thermal discontinuity in well test analysis. Journal of Petroleum Tecnnology (June, 1981), V. 33, No. 6, p. 1095-1105.

Narasimhan, T. N. and Juprasert, S., 1978. Reservoir simulation. In Geothermal resource and reservoir investigations of U.S. Bureau of Reclamation Leasholds at East Mesa, Imperial Valley, California, Howard et al., eds., Lawrence Berkeley Laboratory report, LBL-7094, p. 75-163.

Tsang, Y. W. and Tsang, C. F., 1978. Analytic study of geothermal reservoir pressure response to cold water reinjection. In Proceedings Fourth Workshop on Geothermal Reservoir Engineering Stanford University, Stanford, California, p. 322-331.

van de Kamp, P. C., Howard, J. H., and Graf, A. N., 1978. Geology. In Geothermal reserouce and reservoir investigations of U.S. Bureau of Reclamation Leaseholds at East Mesa, Imperial Valley, California, Howard et al., eds., Lawrence Berkeley Laboratory report, LBL-7094, p. 1-32.

This report was done with support from the Department of Energy. Any conclusions or opinions expressed in this report represent solely those of the author(s) and not necessarily those of The Regents of the University of California, the Lawrence Berkeley Laboratory or the Department of Energy.

Reference to a company or product name does not imply approval or recommendation of the product by the University of California or the U.S. Department of Energy to the exclusion of others that may be suitable.

*TECHNICAL INFORMATION DEPARTMENT*
*LAWRENCE BERKELEY LABORATORY*
*UNIVERSITY OF CALIFORNIA*
*BERKELEY, CALIFORNIA 94720*